The Open Agriculture Journal
DOI: 10.2174/0118743315496436260827112304, 2026, 20, e18743315496436
ISSN: 1874-3315

RESEARCH ARTICLE **OPEN ACCESS**

Crop-aligned Agrivoltaic Design for Semi-arid and Mediterranean Türkiye: Simulated PPFD Suitability Under A- and V-Shaped Bifacial PV Layouts

Duygu Kuzyaka[1,*], Dilan Kılınçoğlu[2], Hüseyin Doğukan Şahin[2], Ömer Yalçın[1] and Talat Özden[1]

[1]*Integrated PV Department, The Center for Solar Energy Research and Applications, Ankara, Türkiye*
[2]*Physics Department, ODTÜ Teknokent, Ankara, Türkiye*

Abstract:
Agrivoltaic (AgriPV) systems enable the co-production of food and electricity, but effective design requires matching crop-specific light requirements to local climate and structural configuration. This study evaluated how PV structural typology and cover ratio jointly shape under-panel light conditions across two climatically contrasting Turkish sites: Harran (hot semi-arid, BSh) and Manavgat (warm-Mediterranean, Csa). Two bifacial PV layouts, A-shaped (ridge) and V-shaped (valley), were simulated at cover ratios of 35%, 50%, and 60%. Using Rhinoceros 3D with Ladybug Tools, hourly ground-level irradiance was simulated and converted to photosynthetic Photon Flux Density (PPFD). Monthly PPFD was sampled at one open-sky reference and five under-panel points; spatial means, standard deviations, coefficients of variation, and leave-one-point-out sensitivity were calculated. Increasing cover ratio systematically reduced PPFD, while V-shaped layouts consistently showed lower spatial dispersion than A-shaped layouts. Monthly spatial standard deviations ranged from 42.4–297.1 μmol/ m^2s in Manavgat and 46.3–376.2 μmol/m^2s in Harran. Simulated light compatibility was strongest for avocado at 35–50% cover ratio, coffee at 50–60%, black cumin at 35–50%, and saffron at 50–60%, with V-frames providing more uniform shading. These findings show that structural typology and cover ratio jointly modulate PPFD suitability and spatial uniformity, offering a practical, preliminary framework for site-specific AgriPV design; rainwater-harvesting channels emerged as a compatible structural co-benefit. Deterministic simulation assumptions, fixed spectral conversion, limited sampling points, and the absence of field validation constrain direct agronomic conclusions. Combining structural typology, cover ratio, and site climate can guide crop-compatible AgriPV design.

Keywords: Agrivoltaics, Bifacial PV, Cover ratio, PPFD analysis, Shading control, High-value crops.

© 2026 The Author(s). Published by Bentham Open.
This is an open access article distributed under the terms of the Creative Commons Attribution 4.0 International Public License (CC-BY 4.0), a copy of which is available at: https://creativecommons.org/licenses/by/4.0/legalcode. This license permits unrestricted use, distribution, and reproduction in any medium, provided the original author and source are credited.

*Address correspondence to this author at the Integrated PV Department, The Center for Solar Energy Research and Applications, Ankara, Türkiye; E-mail: duygu.kuzyaka@odtugunam.org (D.K.)

Cite as: Kuzyaka D, Kılınçoğlu D, Şahin H, Yalçın Ö, Özden T. Crop-aligned Agrivoltaic Design for Semi-arid and Mediterranean Türkiye: Simulated PPFD Suitability Under A- and V-Shaped Bifacial PV Layouts. Open Agric J, 2026; 20: e18743315496436. http://dx.doi.org/10.2174/0118743315496436260827112304

Received: April 15, 2026
Revised: June 24, 2026
Accepted: July 08, 2026
Published: September 14, 2026

Send Orders for Reprints to
reprints@benthamscience.net

1. INTRODUCTION

The integration of agriculture and PVs, termed AgriPVs, represents a paradigm shift in land management, offering the potential to optimize resource utilization and enhance both food and energy production. Traditional agricultural practices often compete with solar energy installations for land, leading to conflicts over land use and potential reductions in agricultural output. AgriPV systems, however, are designed to create mutually beneficial relationships between crops and solar panels, maximizing land efficiency and promoting sustainable resource management [1-3]. This innovative approach involves strategically integrating solar panels into agricultural landscapes, allowing for simultaneous crop cultivation and electricity generation. The design and implementation of AgriPV systems require careful consideration of factors such as crop selection, solar panel orientation, spacing, and shading patterns to ensure optimal plant growth and energy production [2, 4]. Furthermore, the selection of appropriate plant species for AgriPV systems is crucial for maximizing the synergistic benefits of this integrated approach. Designing single-axis-tracking AgriPV systems specifically for high-value crops in these regions is essential to improve land-use efficiency and promote sustainable energy and food production [5, 6]. The collective land-use efficiency of dual-use systems, farm-scale roof plan of the PV array *versus* crop-shadowed surface, and positive externalities of the system related to the energy-food-water nexus, environmental factors, and climate adaptation were investigated with experiments and hybrid models by a large body of researchers, which also clearly demonstrate that AgriPV systems can simultaneously increase farm economic value and improve crop yields, water productivity, and resilience against droughts [6, 7]. Several novel designs, such as movable and lift-type tracking systems, have been demonstrated in recent years. Yet, no consensus has been reached for tropical and arid climates where crop growth cycles and requirements, as well as environmental obstacles, are highly dissimilar compared to continental and temperate regions, leaving a large knowledge gap critical to climate-change resilience and energy-food synergies for developing countries [8, 9]. Designing AgriPV systems involves consideration of several key parameters, including site selection, system configuration, and crop selection, particularly for high-value crops in tropical and arid regions. Site selection is critical, with factors such as solar irradiance, soil quality, and water availability affecting system success. System configuration requires optimization of panel height, spacing, and orientation to balance energy generation and crop yield. Crop selection focuses on identifying high-value species that thrive under partial shading in tropical and arid climates [10, 11]. High-value, shade-tolerant crops represent attractive candidates for AgriPV systems, primarily in tropical and arid regions [11]. Cultivating crops beneath solar panels while simultaneously generating electricity offers a pathway toward a sustainable energy-farming integration well-suited to such climatic conditions. AgriPV innovation chiefly aims to ensure the co-production of clean energy and agricultural supplies on a single land area with minimal output compromise [12]. Designing these systems involves careful consideration of morphological and agronomical aspects, including crop growth habit, shade tolerance, site climate, and additional factors. Diversity in yield responses across crops to shading, from strongly negative through mild-negative to neutral and even positive, depends on species and variety, underscoring the importance of strategic crop selection [6]. Meeting market demand, high-margin products serve as prime candidates for AgriPV cultivation. Practical AgriPV implementations in tropical environments enable the microclimate to be optimized for crop growth, thus achieving significant yield increases while concurrently generating electricity. One 12-month trial demonstrated that the microclimate optimization provided by the AgriPV system increased fresh quality by 11.2% and decreased irrigation compared with open-air conditions [6]. These outcomes depend on identifying specific plant requirements, carefully configuring solar-panel arrays, and adjusting shading to ensure natural sunlight is reduced to the optimal levels for each crop or variety. An example from the poultry sector illustrates how the adoption of such a system in standalone frameworks allows for the simultaneous generation of multiple types of energy. AgriPV installations in arid regions produce effects similar to those observed at tropical installations [11]. Crops can be cultivated in shaded areas, while the reduction in incoming solar irradiation diminishes transpiration rates on the soil, thereby enhancing water resource efficiency. All the benefits observed in tropical systems persist in arid projects along with additional advantages specific to arid climates. Mechanical resistance to storms and sand accumulation is therefore of paramount importance. The key issue in this context lies within the system configuration: optimized arrangements and precise spatial planning are essential to ensure that all underground crops receive the required solar irradiation, since too much shading can adversely affect the plants. AgriPV systems enhance the sustainability of agricultural production through simultaneous and independent food and energy harvesting on the same land, without any tradeoff between the two outputs. Several applications have been reported demonstrating that stair-like or vertical panel configurations can facilitate hybrid field cultivations. For example, a mango plantation with specially designed vertical AV racks in an Indian desert showed improved irrigation and harvest, and 19% of total irrigation water was saved when a shade-tolerant variety of lettuce was cultivated under elevated solar panels in combination with protective nets in an agroecosystem in the Negev desert. Common system failures include partial shading of the PV modules and damage by strong turbulence and surges resulting from high wind speeds during sandstorms [11]. An elevated PV array increases wind velocity and induces a vortex around the supporting framework. Moreover, sand particles removed from the desert floor by accelerated wind velocity may collide and erode the metallic parts of the structural frame. Greater heights, longer spans, and fewer central columns provide more crop-growing area under the installation and better access at the same time. Arid areas are often rich in high-value crops, particularly horticultural products. However, complex climatic factors restrict the growth of many crops [11]. Incorporating PV panels into agricultural land offers opportunities to address environmental and economic challenges and promote sustainable development. AgriPVs, which simultaneously utilize agricultural land for PV power generation and crop cultivation, represent a promising avenue for future initiatives. High-value crops in arid and tropical regions have been proposed as prime candidates for AgriPV systems. Vegetables, forage crops, flowers, energy crops, and fruit trees have been identified for AgriPV cultivation in arid regions. High-value vegetables such as tomatoes, eggplants, zucchinis, lettuce, spinach, strawberries, and blueberries, along with grass, clover, alfalfa, and other forage crops, have been selected based on their economic value and growth characteristics. Sun-demanding flowers, energy crops like Jatropha and Pongamia, and Eucalyptus trees are also suitable. Crop selection further depends on the desired power output of the PV system [6]. Successful AgriPV deployments serve as case studies of high-value crops cultivated under partial shading by solar modules. These systems demonstrate improved efficiency in food production and energy conversion, thereby advancing sustainability. Notable examples include tomato farming in Kerala, India, where profits increased by approximately 25% compared to traditional tomato cultivation and alternative crops. In Aragon, Spain, the cultivation of Gila melons beneath fixed-tilt PV panels yielded 42% more biomass than in open-air greenhouses on an equivalent area. Soft-fruit production in Cambridge, New Zealand, realized a 20% production increase under poly-tunnels integrated with solar arrays while simultaneously supplying electricity for irrigation. In Saint Jean d'Angély, France, a solar park hosting strawberries and asparagus reported a 60% uptick in revenue compared to a nearby open-air field. In warm-humid climates, June-bearing strawberries cultivated in Maui, Hawai'i, produced 80% more fruit under solar panels and significantly increased the number of marketable berries by mitigating fungal diseases prevalent in humid conditions. Technical design innovations, including solar-tracking, vertical, and bifacial PV panel configurations, enhance performance in high-irradiance environments. Mechanical design specifications and material selection for PV racking that can accommodate tall, trellis-based crops provide structural resiliency while respecting local environmental constraints [11]. The selection of high-value crops was guided by their economic importance, adaptability to regional climates, and specific requirements for Photosynthetic Photon Flux Density (PPFD). In this study, AgriPV systems integrate PV panels with crop cultivation, providing partial shading in semi-arid and warm-Mediterranean areas. In arid regions, the Harran Plain was chosen as a representative site due to its semi-arid climate, characterized by high solar irradiance, limited rainfall, and extreme temperatures that challenge conventional agriculture [13]. For this location, saffron (Crocus sativus) and black cumin (*Nigella sativa*) were selected as target crops. Saffron, one of the world's most valuable spices, demonstrates optimal growth under moderate shading, with PPFD requirements ranging from 200 to 400 μmol/m^{2}s [14-16]. Black cumin, a medicinal crop with rising global demand, is responsive to light conditions, particularly during germination and early establishment [17]. For the present screening analysis, a provisional PPFD target range of 350–500 μmol/m^{2}s was adopted and should be validated experimentally under AgriPV conditions [17, 18]. Both crops are well-suited to arid conditions, where controlled shading provided by AgriPV systems can mitigate excessive heat stress while ensuring sufficient light for photosynthesis. For warm-Mediterranean climates, Manavgat in southern Türkiye was selected as a case study site, given its mild winters, dry-hot summers, and high solar potential [19]. Avocado (*Persea americana*), a high-value fruit with expanding markets, was chosen due to its preference for moderate to high irradiance, with PPFD requirements in the range of 400–700 μmol/m^{2}s [20, 21]. Coffee (Coffea arabica), one of the most globally traded commodities, was also included as an experimental candidate given recent niche-market trials in subtropical Turkish provinces, as it performs optimally under partially shaded environments with PPFD values between 200 and 400 μmol/m^{2}s [22-24]. The integration of these perennial crops into AgriPV designs enables simultaneous renewable energy production and crop cultivation, yielding strong economic potential. By matching PV system designs to the PPFD requirements of these high-value crops, this research lays the groundwork for crop-specific AgriPV designs in different climatic regions. The approach seeks to improve land-use efficiency, climate adaptation, and agricultural resilience in semi-arid and warm-Mediterranean areas. Different structural designs of AgriPV systems have been suggested in the literature, such as fixed-tilt monofacial arrays, single-axis trackers, vertical bifacial panels, movable or lift-type systems, and different gable or channel-based configurations [5, 6, 11, 12]. In this research, A-shaped (ridge-type) and V-shaped (valley-type) structural typologies were chosen for a few reasons that are in accordance with the objectives of growing high-value crops under partial shading. The A-frame design, like a classic gable roof, provides natural structural stability, effective rainwater runoff through double eave gutters, and easy maintenance access. This geometry generates separate lateral shade lobes that can be oriented with crop rows to generate variable light micro-environments. V-shaped (valley in the middle) creates a more uniform shading corridor under the array, good for shade-tolerant crops that need consistent light reduction. This arrangement inherently provides a central gutter for rainwater harvesting, minimizes dust accumulation on modules due to better airflow, and is expected to support rear-side irradiance gains through enhanced ground-reflected radiation, a potential bifacial advantage that warrants quantification in future energy yield studies. Both typologies were selected for their suitability for integrated rainwater harvesting, a key co-benefit in arid and seasonally dry areas. Moreover, their geometric adaptability enables fine-tuning of ground coverage ratio (CR) and sub-panel light distribution to achieve species-specific PPFD targets. These designs therefore provide a pragmatic trade-off between agricultural light management, structural compatibility with bifacial PV modules, and hydraulic resource efficiency, addressing a critical gap in AgriPV deployments for semi-arid and warm-Mediterranean climates. Despite the growing body of AgriPV literature, a clear research gap remains early-stage design frameworks that explicitly link PV structural geometry and cover ratio to crop-specific PPFD requirements under contrasting dry-climate regimes are scarce, particularly for high-value specialty crops in Türkiye. Most existing studies focus on temperate European conditions and do not address the combinatorial effect of typology (A- *vs.* V-frame) and cover ratio on sub-panel light uniformity across different Köppen climate classes. The present study advances AgriPV research by (i) developing a simulation-based, crop-aligned design framework for two structurally distinct PV typologies at three cover ratios across two climatically contrasting Turkish sites; (ii) evaluating PPFD compliance for four high-value crops, saffron, black cumin, avocado, and coffee, against species-specific target bands; and (iii) identifying typology-dependent shading signatures (lateral lobes for A-frames *vs.* central corridor for V-frames) that can guide spatial crop allocation. The central hypothesis is that moderate cover ratios (CR = 35–60%) combined with appropriate typology selection can maintain sub-panel PPFD within agronomically compatible ranges for all four target crops across both sites, without necessitating active shading control.

2. MATERIALS AND METHODS

2.1. Site Selection

Within Türkiye, contrasting climate regimes such as the Harran Plain's hot semi-arid steppe (Köppen BSh) and Manavgat's warm-Mediterranean climate (Köppen Csa) illustrate how classifications shape agricultural and energy potential [25, 26]. The locations of the two study sites are presented on a map of Türkiye, indicating Antalya and Şanlıurfa provinces, within which the Manavgat and Harran districts are situated, respectively (Fig. **1**).

The two study sites were selected to represent contrasting dry-climate regimes within Türkiye: the Harran Plain in Şanlıurfa Province (southeastern Türkiye) and the Manavgat district in Antalya Province (southern Türkiye). Their locations are shown on the map of Türkiye in Fig. (**1**). Harran is situated at approximately 36.87°N, 39.02°E, at an elevation of 465 m above sea level, and is classified as a hot semi-arid steppe climate (Köppen BSh). The region receives a mean annual precipitation of approximately 365 mm, concentrated in the winter months, with negligible rainfall from June through September. Mean annual temperature is approximately 18.5°C, with summer maxima regularly exceeding 40°C. Annual global horizontal irradiance (GHI) is approximately 1,950 kWh m^{-2} yr^{-1}, corresponding to roughly 2,993 sunshine hours per year, making it one of the highest solar-resource zones in Türkiye. These conditions, intense summer radiation, high evaporative demand, and low seasonal water availability, create substantial stress for conventional open-field agriculture and motivate the evaluation of AgriPV shading strategies for drought-tolerant, high-value crops such as saffron and black cumin. Manavgat is located at approximately 36.78°N, 31.44°E, at an elevation of approximately 20 m above sea level and is classified as a warm-Mediterranean climate (Köppen Csa). Annual precipitation averages approximately 1,020 mm, distributed predominantly across the autumn–winter season, while summers are characteristically hot and dry. Mean annual temperature is approximately 19.2°C. Annual GHI is approximately 1,860 kWh m^{-2} yr^{-1}, with approximately 3,000 sunshine hours per year. The combination of high solar resource, mild winters, and seasonal aridity positions Manavgat as a suitable candidate for AgriPV integration with perennial, shade-tolerant, high-value crops including avocado and coffee.

Fig. (1). Location of the study sites: Antalya and Şanlıurfa provinces, encompassing the Manavgat and Harran districts, respectively, shown on a map of Türkiye.

Climate data for both sites were sourced from the Turkish Meteorological Service (MGM), the SOLARGIS global horizontal irradiance atlas, and EnergyPlus Typical Meteorological Year (TMY) weather files corresponding to the Şanlıurfa and Antalya stations, respectively. Köppen–Geiger climate classifications follow the 2023 updated global dataset. Harran is characterized by very low rainfall and high evaporative demand (long-term mean precipitation ≈277–430 mm yr^{-1}, with station means reported around ~365 mm yr^{-1}), consistent with BSh conditions and favorable for AgriPV strategies that mitigate heat and soil-moisture stress [27, 28]. In contrast, Manavgat (Antalya Province) has rainy, mild winters and very dry, hot summers typical of Csa, with ~960–1,080 mm yr^{-1} precipitation and ~3,000 annual sunshine hours, alongside nationally high solar resource mapped for the Mediterranean coast [26, 29, 30]. These climatic contrasts guided our case-study crop choices and design targets: drought-tolerant, high-value saffron and black cumin in Harran; and avocado and coffee, perennials suited to winter-wet, summer-dry regimes with strong irradiance, in Manavgat. The pairing underscores Türkiye's climate diversity and the need for site-specific AgriPV designs that align PV layout and shading with local water balance and crop physiology.

2.2. Crop Selection

Avocado and coffee were selected for the Manavgat region, while black cumin (Nigella sativa) and saffron (Crocus sativus) were chosen for Harran, based on their agricultural relevance, site-specific climatic suitability, and growing economic interest. Avocado cultivation has expanded significantly in southern Türkiye, particularly in Antalya province, due to its subtropical climate and increasing domestic demand. Coffee, though not commercially produced at scale in Türkiye, was included as a forward-looking candidate: its PPFD requirements (200–400 μmol m^{-2} s^{-1}) are well-matched to the shaded micro-environments produced by AgriPV structures, and limited experimental trials of Coffea arabica cultivation under controlled or protected conditions in subtropical provinces such as Antalya and Rize demonstrate proof-of-concept feasibility [31]. As AgriPV structures effectively moderate temperature extremes and reduce peak irradiance, they may expand the thermal envelope for coffee cultivation in Manavgat beyond what open-field conditions currently permit. The inclusion of coffee therefore represents a scenario-based assessment of its light compatibility under AgriPV shading, rather than a reflection of current regional production. For the Harran site, black cumin was selected for its well-established adaptability to semi-arid conditions and its growing significance in pharmaceutical and culinary markets, while saffron was included due to its high economic value and cultivation potential under controlled irrigation. Production data from the Turkish Statistical Institute (TÜİK) portal confirm the availability of regional statistics for avocado and black cumin between 2022 and 2024, reported in metric tons [32]. However, no regional production data were available for coffee or saffron within the same period, consistent with their status as experimental or niche crops at these locations. Figure **2** illustrates the recorded production volumes for avocado in Manavgat and black cumin in Harran, alongside their relative contributions to provincial totals.

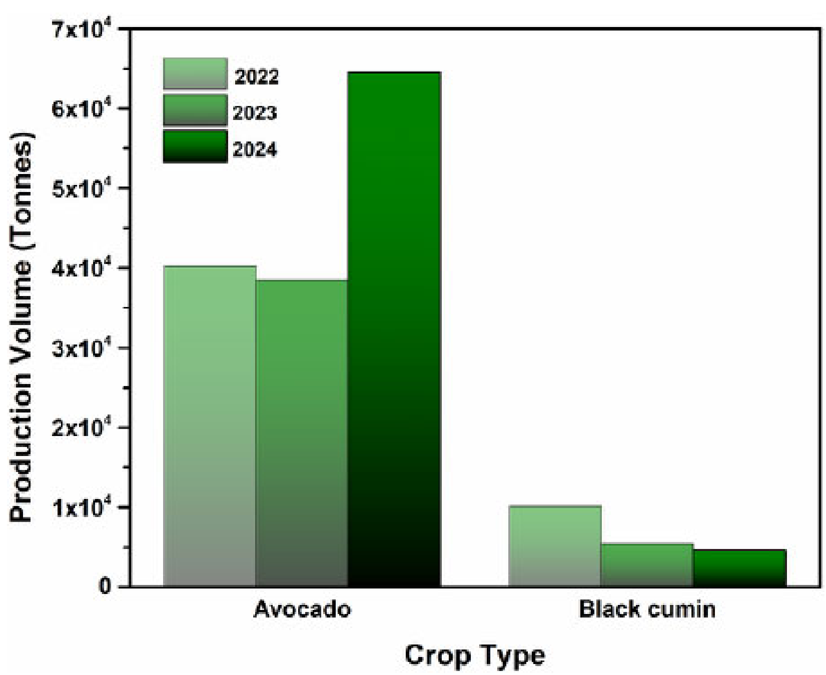

Fig. (2). Production volumes of Avocado and black cumin throughout Türkiye.

Although Türkiye is globally known for its coffee culture, particularly Turkish coffee, the country is not a coffee producer due to its non-tropical climate. Coffee cultivation requires consistent high temperatures and humidity, conditions that are not naturally met in most Turkish regions. However, there have been limited experimental trials of Coffea arabica cultivation under controlled environments in subtropical provinces like Antalya and Rize, though no large-scale commercial production exists to date [31]. In contrast, Türkiye is one of the few European countries where saffron (*Crocus sativus*) is traditionally and commercially cultivated. The town of Safranbolu in Karabük Province serves as the main production hub, where high-value saffron is grown under temperate continental conditions, characterized by dry summers and cold winters. Saffron production remains labor-intensive and small-scale, yet it holds significant cultural and economic value [33].

The species selected for this study, avocado, coffee, saffron, and black cumin, are all high-value crops. Notably, they require relatively low PPFD values for growth, as shown in Table **1** [16, 18, 21, 24].

This characteristic makes them relatively advantageous for cultivation under shading conditions, such as those created by AgriPV system designs.

Table 1. PPFD requirements of avocado, coffee, saffron, and black cumin.

Crop Name	PPFD Requirement (μmol/m^{2}s)
Avocado (*Persea americana*)	400-700
Coffee (*Coffea arabica*)	200-400
Saffron	200-400
Black Cumin	350-500

2.3. System Design

An approach was adopted to assess the light-environment feasibility of an AgriPV system tailored for high-value crops, avocado, coffee, saffron, and black cumin, in Manavgat and Harran. Geographical Information Systems (GIS) were used to characterize site-specific climatic contexts. The AgriPV layout was theoretically designed in two structural variants: an A-shaped frame and a V-shaped frame, each mounting standard bifacial c-Si modules. Both variants were dimensioned to meet species-specific PPFD setpoints through the coordinated selection of tilt (θ), inter-row spacing (S), ridge/valley height (h), and coverage ratio (CR), while preserving under-panel clearance for farm operations. The simulations assumed standard bifacial c-Si modules (dimensions: 2.0 m × 1.0 m; bifaciality factor: 0.70) with an under-panel clearance height that was parametrically adjusted per scenario to achieve the target cover ratios while preserving agricultural access. The specific clearance heights, row spacings, and module count for each configuration (A-shaped *vs.* V-shaped and each CR level) are summarized later in this section. Tilt angles and interrow pitches were coordinated to meet species-specific PPFD setpoints; a uniform tilt of 35° was applied across all scenarios. This study evaluated two structural typologies: an A-shaped layout, in which standard bifacial c-Si modules are mounted on paired inclined planes forming a ridge (Fig. **3**), and a V-shaped layout, in which modules form a central valley (Fig. **4**).

The geometries also enable rainwater harvesting: the V-shaped arrangement incorporates a central valley gutter that collects runoff and conveys it to storage (*e.g.*, header tanks or subsurface cisterns), whereas the A-shaped arrangement uses dual eave gutters along the outer edges to capture and route precipitation. Harvested water can be fed to drip/micro-irrigation lines or used for module cleaning, reducing both irrigation demand and dust-related optical losses.

Fig. (3). Schematic view of an A-shaped AgriPV structure.

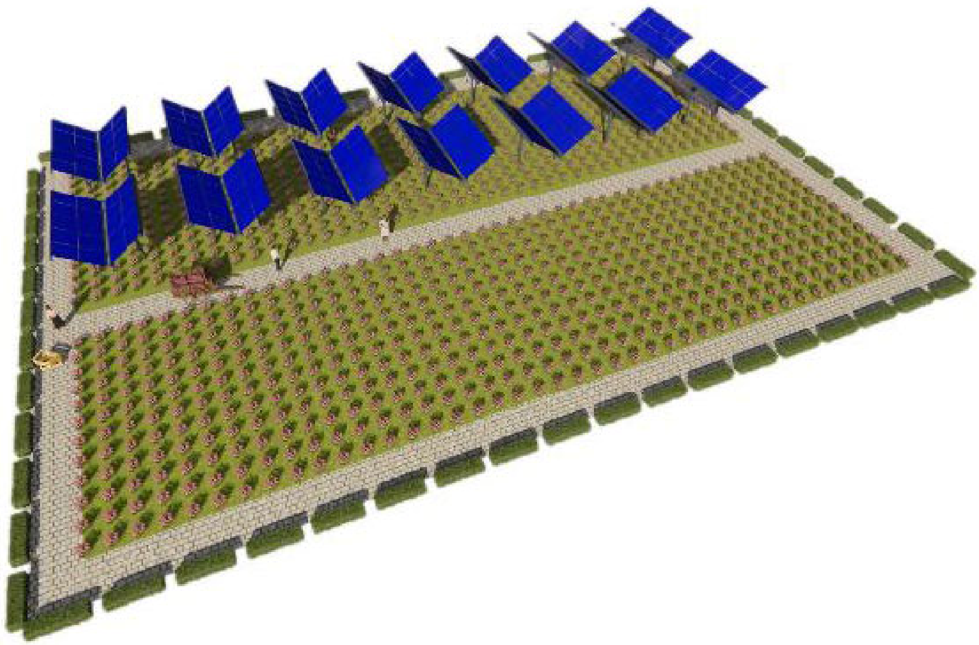

Fig. (4). Schematic of a V-shaped AgriPV structure.

From a climatic-fit perspective, the BSh Harran design prioritizes shading to moderate panel temperature and evapotranspiration, coupled with larger gutter cross-sections to exploit infrequent but intense rain events; the Csa Manavgat design emphasizes winter peak rainfall management and summer water buffering. Structurally, the A-shaped variant offers high lateral stiffness and efficient debris shedding, while the V-shaped variant facilitates rear-side irradiance gains through controlled ground reflectance and provides a protected corridor for cables and irrigation manifolds. In both cases, the layout is parametrically tuned so that seasonal light availability remains within target bands (*e.g.*, coffee ~200–400, avocado ~400–700, saffron ~200–400, black cumin ~350–500 μmol m^{-2} s^{-1}), enabling crop-aligned light management; quantitative assessment of PV energy yield is beyond the scope of this simulation study and is recommended for future work.

For each typology, we analyze three CR, 35%, 50%, and 60%, yielding a 2×3 scenario matrix that disentangles the effect of geometry (A *vs.* V) from shading intensity (CR levels). Here, the CR is defined as the plan-view PV footprint relative to the plot area, controlled *via* tilt, module row width, and inter-row pitch. Both frames are configured to (i) maintain agricultural clearance beneath the array, (ii) align with species-specific PPFD set-points through parametric spacing/tilt selection, and (iii) allow rainwater-harvesting integration. In the V-shaped layout, a central valley gutter captures runoff for storage and distribution; in the A-shaped layout, dual eave gutters collect precipitation along the outer edges. The CR35 setting represents a sparse panel suited to higher light-demand crops, CR50 a balanced shading regime, and CR60 a denser panel structure favoring shade-tolerant species; across all cases, the layouts are tuned so that sub-panel PPFD remains within target bands for avocado, coffee, saffron, and black cumin. This scenario design may enable a consistent comparison of light environment, potential water savings *via* harvested rainfall, and the geometric suitability of contrasting structural solutions for bifacial module integration, with quantitative PV energy assessment left for future work. Table **2** summarizes the comparative scenario matrix for A-shaped and V-shaped AgriPV frames configured with standard bifacial c-Si modules at the Harran (BSh) and Manavgat (Csa) sites across three CRs (CR = 35, 50, 60), including species-specific PPFD targets, integrated rainwater harvesting, and key parametric variables.

The matrix compares A- and V-shaped layouts at CR = 35/50/60 for Harran and Manavgat, calibrated to species-specific PPFD bands and incorporating rainwater-harvesting gutters. CR levels are chosen to maintain PPFD within target ranges for each crop, while the V-frame supports bifacial rear-side gains through optional ground-albedo management.

Across all simulated scenarios, a uniform tilt angle of 35° was applied. The PV modules used in the simulations had dimensions of 225 mm × 1134 mm × 6 mm, and an azimuth range of −90° to +90° was considered to account for east–west orientations. The total simulated ground area was 561 m^2 in all cases. Additional design parameters employed in the simulations are listed in Table **3**.

Table 2. Scenario matrix for crop-aligned AgriPV designs using A-shaped and V-shaped frames with bifacial c-Si modules at Harran and Manavgat under three cover ratios (CR = 35/50/60).

ID	Typology	CR (%)	Shading Regime	Gutter Type	Target Crops
H-A-35	A-shaped	35	Low	Dual eave gutters	Saffron; Black cumin
H-A-50	A-shaped	50	Moderate	Dual eave gutters	Saffron; Black cumin
H-A-60	A-shaped	60	High	Dual eave gutters	Saffron; Black cumin
H-V-35	V-shaped	35	Low	Central valley gutter	Saffron; Black cumin
H-V-50	V-shaped	50	Moderate	Central valley gutter	Saffron; Black cumin
H-V-60	V-shaped	60	High	Central valley gutter	Saffron; Black cumin
M-A-35	A-shaped	35	Low	Dual eave gutters	Avocado; Coffee
M-A-50	A-shaped	50	Moderate	Dual eave gutters	Avocado; Coffee
M-A-60	A-shaped	60	High	Dual eave gutters	Avocado; Coffee
M-V-35	V-shaped	35	Low	Central valley gutter	Avocado; Coffee
M-V-50	V-shaped	50	Moderate	Central valley gutter	Avocado; Coffee
M-V-60	V-shaped	60	High	Central valley gutter	Avocado; Coffee

Table 3. Key geometric input parameters for the simulated AgriPV scenarios under different configurations (A-shaped *vs.* V-shaped).

ID	Row Spacing (m)	Under-panel Clearance Height (m)	Number of Modules Per Scenario
H-A-35	12.36	3.28	80
H-A-50	7.20	3.28	120
H-A-60	6.21	3.28	140
H-V-35	12.36	2.25	80
H-V-50	7.42	2.25	120
H-V-60	6.27	2.25	140
M-A-35	12.36	3.28	80
M-A-50	7.20	3.28	120
M-A-60	6.21	3.28	140
M-V-35	12.36	2.25	80
M-V-50	7.42	2.25	120
M-V-60	6.27	2.25	140

3. SIMULATION WORKFLOW AND LIGHT DISTRIBUTION ANALYSIS

The analytical assessment focuses on two key aspects: (i) ground-level solar irradiance distribution and (ii) photosynthetic photon flux density (PPFD) distribution and crop light compatibility assessment.

3.1. Solar Irradiance and Shading Analysis

Ground-level solar distribution was evaluated using Ladybug Tools (version 1.7.0) and Honeybee extensions within the Rhinoceros 3D / Grasshopper parametric environment (Rhinoceros 7, McNeel). Simulations employed a Reinhart sky model (subdivisions: MF = 1) with hourly direct and diffuse radiation components from EnergyPlus Weather (EPW) files sourced from the EnergyPlus climate data repository: the Şanlıurfa station EPW was used for Harran (representing BSh conditions) and the Antalya station EPW for Manavgat (representing Csa conditions); both files cover a Typical Meteorological Year (TMY) period. The ground plane was discretized at a mesh resolution of 0.5 m, and irradiance was calculated at a height of 0.1 m above ground level to represent in-field sensor conditions. The ground solar radiation map in Ladybug (within Rhinoceros) computes hourly solar irradiance distribution using both geometric and climatic inputs. Ground-level total irradiance (G_{total}) is the sum of direct beam (G_{beam}), diffuse ($G_{diffuse}$), and ground-reflected ($G_{reflected}$) components. These components were computed by Ladybug Tools' ray-tracing routine for each hourly time step and mathematically expressed in Eq. (**1**).

$$G_{total} = G_{beam} + G_{diffuse} + G_{reflected} \quad (1)$$

The ground solar radiation map in Ladybug (within Rhinoceros) computes hourly solar irradiance distribution using both geometric and climatic inputs. The total irradiance on the ground surface is given by Eq. (**1**). Hourly G_{total} values were then averaged over daylight hours to obtain monthly mean irradiance (Wm^{-2}), which was subsequently converted to PPFD using a conversion factor of 4.57 µmol J^{-1} [34]. No annual energy yield was computed, as this study focuses solely on light availability for crops.

3.2. PPFD Conversion and Crop Suitability Assessment

The available solar radiation was converted into PPFD (µmol m^{-2} s^{-1}) using a conversion factor of 4.57 µmol J^{-1} to transform monthly mean irradiance (W m^{-2}) into photon flux density. This factor relates the energy of photons in the photosynthetically active radiation (PAR, 400–700 nm) waveband to their molar count under a solar spectrum [34]. It should be noted that this factor is derived for standard solar radiation and represents an approximation; spectral shifts under panel shading may alter the effective conversion slightly. Monthly irradiance values extracted at each sampling point (Whm^{-2} per month) were first converted to time-averaged W m^{-2} over daylight hours and then multiplied by 4.57 to obtain mean PPFD estimates. These values were compared against species-specific thresholds for the four target crops: avocado (400–700), coffee (200–400), saffron (200–400), and black cumin (350–500 μmol m^{-2} s^{-1}), to assess whether the simulated light environments fall within agronomically acceptable ranges.

4. RESULTS

Results were synthesized for A-shaped and V-shaped AgriPV layouts at Harran and Manavgat across three CRs (CR = 35, 50, 60; see Table **2**). Sub-panel PPFD distributions were compared with species-specific thresholds, avocado 400–700, coffee 200–400, saffron 200–400, and black cumin 350–500 μmol m^{-2} s^{-1}, and were evaluated for seasonal suitability and spatial homogeneity both along and between rows. PV metrics were then examined, including plane-of-array irradiance, typology-dependent bifacial gain, and shading/mismatch effects associated with CR. Finally, design trade-offs were analyzed, and site-specific recommendations were defined, accompanied by a discussion of model assumptions and limitations. For both typologies (A-shaped and V-shaped), row spacing was arranged to create crop alleys and service access, to achieve the target CRs (CR = 35, 50, 60), and to maintain species-specific PPFD bands. It is likely to integrate rainwater-harvesting hardware into the geometry. Outer eave gutters were specified for the A-shaped frames, and a continuous valley gutter was specified for the V-shaped frames, with conveyance to storage for redistribution. Cable and irrigation routing were accommodated within protected corridors (particularly in the V-shaped configuration), and rear-side irradiance gains are expected to be supported through managed ground albedo, whereas the A-shaped configuration facilitates efficient shedding and straightforward maintenance access. To quantify the PPFD delivered to shade-tolerant crops by our proposed design, we employed a computational modeling approach using Rhinoceros 3D with the Ladybug plugin. Solar radiation metrics were gathered from six distinct measurement sites beneath the PV array to facilitate comparative analysis. The initial solar radiation readings were subsequently transformed into PPFD values utilizing established photometric conversion algorithms. This dataset was then employed to simulate the monthly fluctuations in PPFD distribution over an entire annual cycle, thereby assessing the system's influence on light accessibility for the target crops. The simulation incorporated both diurnal and seasonal solar trajectories, thereby ensuring that the results accurately represent authentic agroclimatic conditions. A-shaped and V-shaped AgriPV systems were analyzed for different CRs (35, 50, and 60%) in the Harran district, chosen for its arid conditions, with the corresponding ground solar radiation distribution presented in Fig. (**5**).

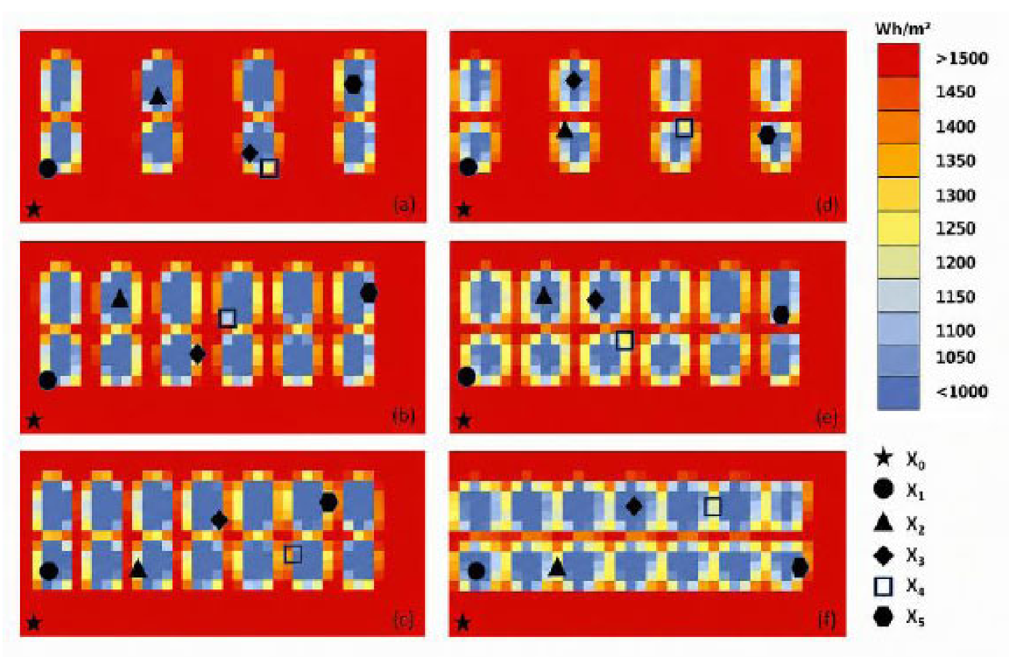

Fig. (5). The ground solar distribution map indicating the pre-determined locations of X1, X2, X3, X4, and X5 of H-A-35 (**a**), H-A-50 (**b**), H-A-60 (**c**), H-V-35 (**d**), H-V-50 (**e**), and H-V-60 (**f**).

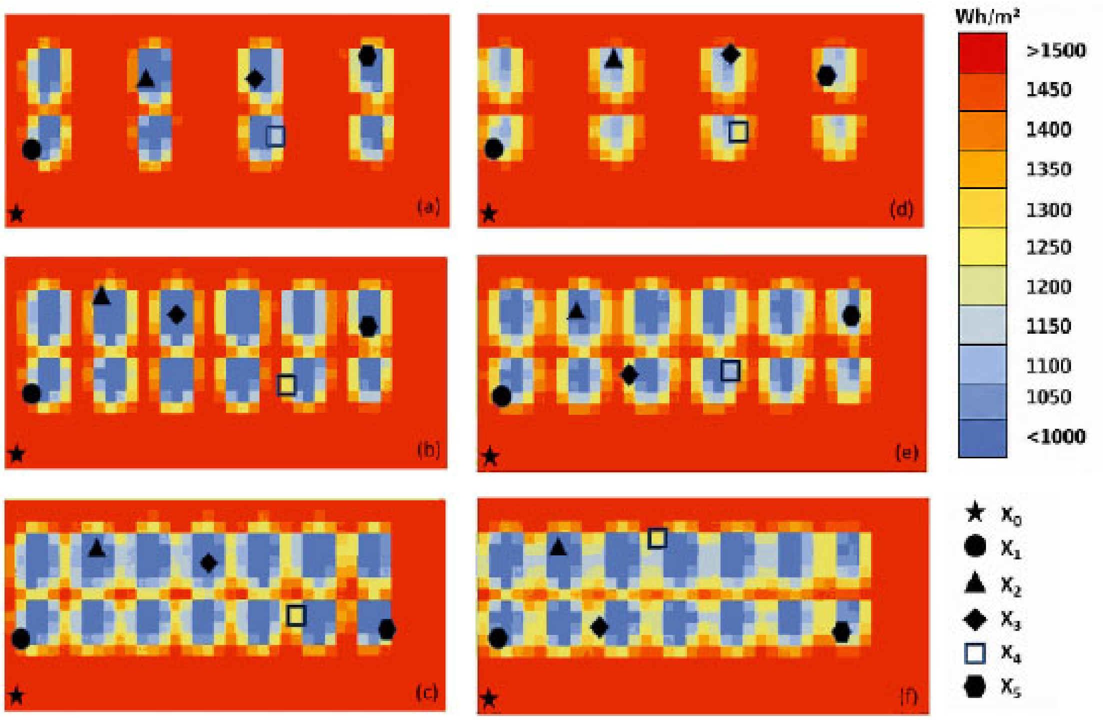

Fig. (6). The ground solar distribution map indicating the pre-determined locations of X1, X2, X3, X4, and X5 of M-A-35 (**a**), M-A-50 (**b**), M-A-60 (**c**), M-V-35 (**d**), M-V-50 (**e**), and M-V-60 (**f**).

For the arid-case site (Harran, BSh), A-shaped and V-shaped AgriPV layouts were simulated at three CRs (CR = 35, 50, 60), and the resulting ground-level cumulative irradiance fields (Wh m^{-2}) were mapped. Panels (a–c) correspond to H-A-35/50/60, and (d–f) to H-V-35/50/60; the color bar spans <1000 to >1500 Wh m^{-2}. As CR increases, the low-irradiance (blue) footprints beneath the arrays expand while high-irradiance perimeter bands contract. In A-shaped layouts, minima are expressed as two lateral shade lobes per bay, whereas in V-shaped layouts, a central valley corridor of reduced irradiance is formed. Pre-defined points X_0–X_5 indicate virtual sampling locations, and through them, ground-irradiance values were extracted. These maps were used to verify that sub-panel light levels at representative positions can be tuned to the species-specific PPFD bands targeted for saffron (200–400 µmol m^{-2} s^{-1}) and black cumin (350–500 µmol m^{-2} s^{-1}).

A-shaped and V-shaped AgriPV systems were analyzed for different CRs (35, 50, and 60%) in the Manavgat district, selected for its warm-Mediterranean (Köppen Csa) conditions, with the corresponding ground solar radiation distribution presented in Fig. (**6**).

For the warm-Mediterranean site (Manavgat, Csa), cumulative ground-plane irradiance (Wh m^{-2}) is mapped for A-shaped layouts at CR = 35, 50, 60 in panels (a–c) and for V-shaped layouts at the same CRs in (d–f); the color scale spans <1000 to >1500 Wh m^{-2}. Increasing CR enlarges the low-irradiance footprints beneath the arrays and narrows the high-irradiance perimeter bands. In A-shaped cases, minima appear as two lateral shade lobes per bay, whereas V-shaped cases exhibit a central valley corridor of reduced irradiance. Pre-defined points X_0–X_5 denote virtual sampling locations in Rhinoceros; irradiance values extracted at these points were used to check that representative sub-panel levels can be tuned to the PPFD targets for avocado (400–700 µmol m^{-2} s^{-1}) and coffee (200–400 µmol m^{-2} s^{-1}).

Across both sites, the ground-irradiance maps show that increasing CR enlarges low-irradiance footprints and narrows high-irradiance perimeter bands; A-shaped arrays generate two lateral shade lobes per bay, whereas V-shaped arrays form a central corridor of reduced irradiance. For Harran (BSh), these patterns indicate that saffron (≈200–400 µmol m^{-2} s^{-1}) is best accommodated at CR50–60 under either typology, with the V-corridor yielding more uniform shading, while black cumin (≈350–500 µmol m^{-2} s^{-1}) is better aligned at CR35–50, as CR60 risks dropping core locations below the lower bound. For Manavgat (Csa), coffee (≈200–400 µmol m^{-2} s^{-1}) is most consistently supported at CR50–60 (particularly in V-frames), whereas avocado (≈400–700 µmol m^{-2} s^{-1}) is favored at CR35–50, with CR60 posing an under-illumination risk. These inferences were drawn from simulated cumulative ground irradiance (Wh m^{-2}) and interpreted with respect to target PPFD bands; therefore, seasonal dynamics and spatial homogeneity should be verified *via* PPFD simulations or field campaigns. On this basis, the scenario-level findings were then evaluated crop by crop. Species-specific PPFD target bands, saffron 200–400, black cumin 350–500, avocado 400–700, and coffee 200–400 µmol m^{-2} s^{-1}, were adopted as evaluation criteria. For Harran (saffron, black cumin) and Manavgat (avocado, coffee), sub-panel PPFD predicted for each A- and V-shaped design at CR = 35/50/60 was sampled at pre-defined locations (X_0–X_5); compliance with the target ranges was then assessed, and the crop-level suitability of each layout was discussed.

For Manavgat, mrepresenting warm-Mediterranean conditions (Köppen Csa) with avocado and coffee, and Harran, representing arid hot semi-arid conditions (Köppen BSh) with black cumin and saffron, crop suitability was evaluated for the six previously defined system configurations (A-shaped and V-shaped frames at CR = 35, 50, 60). For each crop, monthly sub-panel light environments were derived by averaging the ground solar distribution maps each month; for each configuration, irradiance values were extracted at six predefined virtual sampling locations in Rhinoceros (X_0–X_5), comprising one open-sky reference and five under-panel positions. The resulting monthly means were compared with species-specific PPFD target bands to assess compliance and identify the most appropriate configuration for each crop. Crop-wise outcomes are reported sequentially; analyses for avocado are presented in Fig. (7).

Monthly sub-panel PPFD series were derived from the ground-irradiance maps for the six Manavgat configurations (M-A-35/50/60 and M-V-35/50/60) by averaging values at six pre-defined virtual sampling locations (X_0–X_5). The shaded avocado target band (400–700 µmol m^{-2} s^{-1}) was used as the compliance criterion, and the planting window was indicated for seasonal context. Across all cases, the open-sky reference (X_0) rose well above the upper bound in late spring–summer, while under-panel locations (X_1–X_5) reduced PPFD into agronomic ranges. A systematic CR effect was observed: higher CR suppressed PPFD across months, and V-shaped layouts tended to exhibit tighter clustering (*i.e.*, lower spatial dispersion) among X_1–X_5 than A-shaped layouts, reflecting the more uniform shading produced by the central valley corridor.

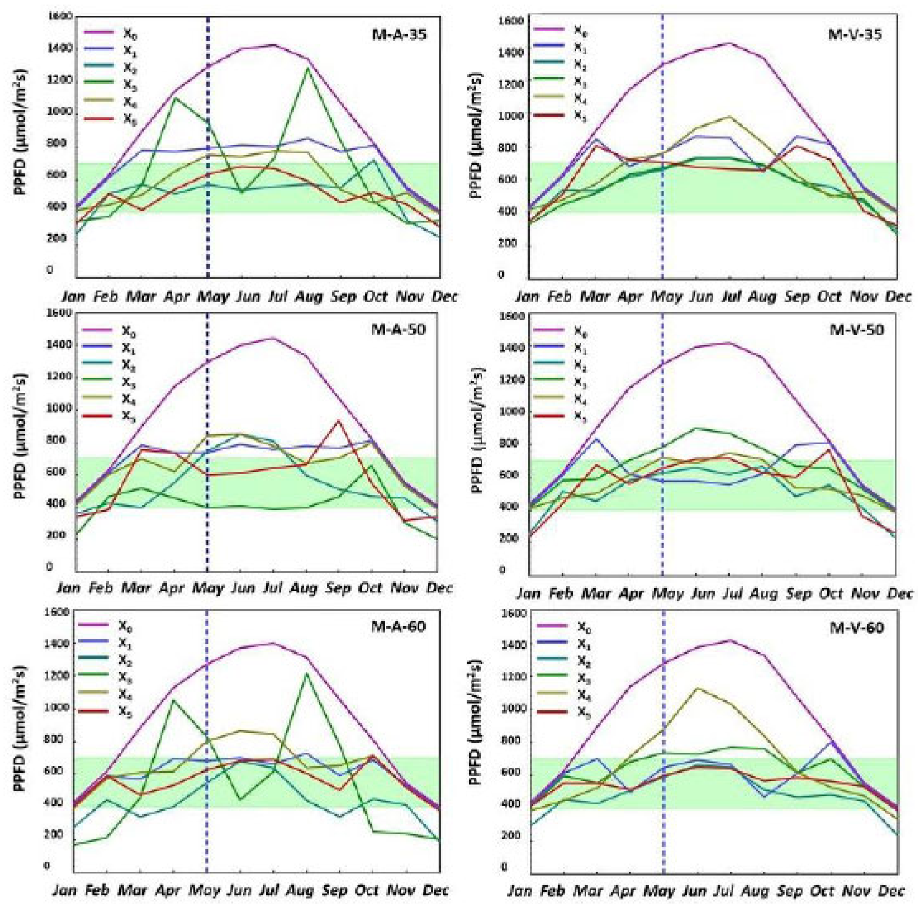

Fig. (7). Monthly sub-panel PPFD (µmol m^{-2} s^{-1}) at six virtual sampling points (X_0–X_5) for M-A-35/50/60 and M-V-35/50/60 (Manavgat site). Shaded band = avocado PPFD target 400–700 µmol m^{-2} s^{-1}; dashed line = avocado planting season. (X_0: open-sky reference; X_1–X_5: under-panel.).

From an agronomic standpoint, the most persistent overlap with the avocado target band was obtained under moderate CRs (CR = 35–50), with V-shaped frames generally sustaining the band for longer portions of the year and around the planting window. Under CR = 60, several traces remained near or below the lower threshold during winter–early spring, implying a higher risk of light limitation unless geometric or optical parameters are adjusted (*e.g.*, reduced effective coverage/greater row pitch, slight tilt recalibration, or controlled ground-albedo enhancement). These results indicate that avocado performance is better supported by moderate shading with spatially uniform sub-panel light, and that high-coverage designs would require compensating measures to maintain PPFD within 400–700 μmol m^{-2} s^{-1}.

Results for coffee are presented in Fig. (**8**), with reference to the PPFD target band (200–400 μmol m^{-2} s^{-1}).

For coffee, monthly sub-panel PPFD series were derived from the ground-irradiance maps by averaging values at six pre-defined virtual sampling locations (X_0–X_5) for each Manavgat configuration (M-A-35/50/60 and M-V-35/50/60). The species-specific target (200–400 μmol m^{-2} s^{-1}) was used as the compliance criterion. Across scenarios, CR = 50–60 generally yielded the most persistent overlap with the target band, particularly in V-shaped layouts, where a central valley corridor produced tighter clustering among under-panel traces, whereas CR = 35 frequently produced exceedances above the upper bound during late spring–summer. At the highest coverage (CR = 60), occasional under-illumination near the lower threshold was observed in winter–early spring, indicating that minor geometric or optical adjustments (*e.g.*, modestly increased row pitch or managed ground albedo) may be warranted for year-round compliance. Overall, coffee suitability was best supported by moderate-to-high coverage with uniform shading, with V-frames offering the most consistent seasonal performance within the 200–400 μmol m^{-2} s^{-1} band.

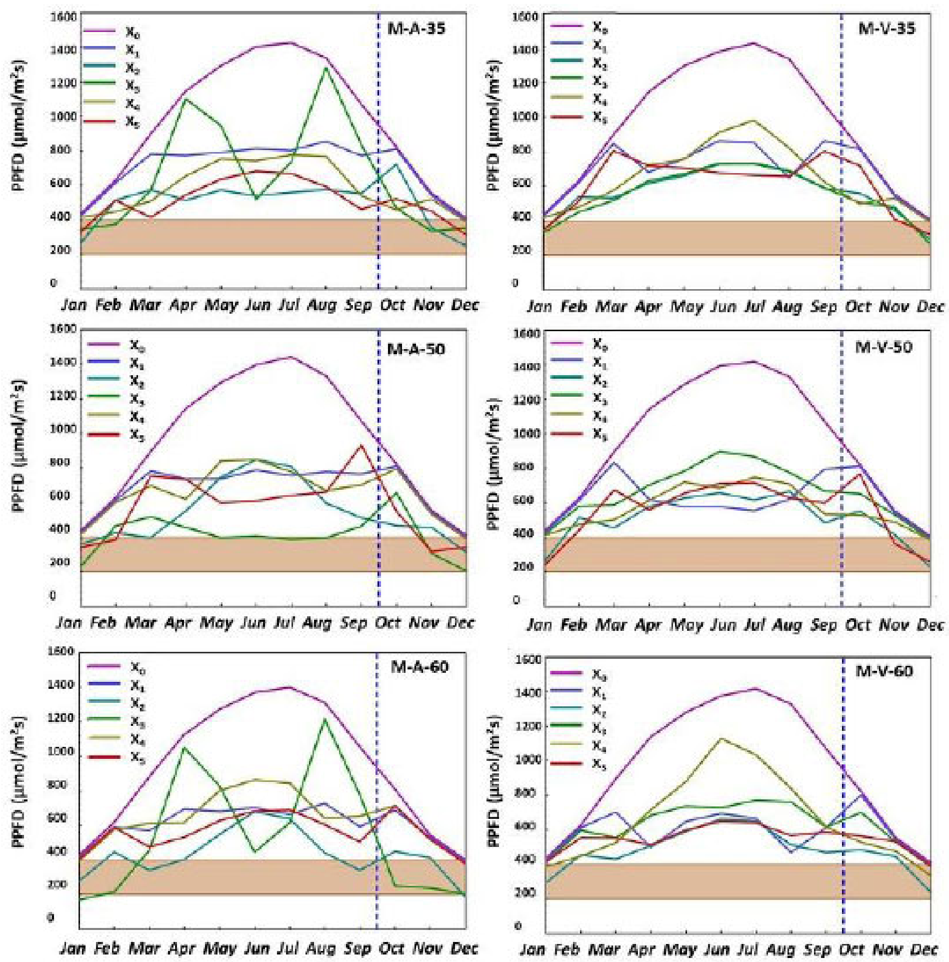

Fig. (8). Monthly sub-panel PPFD (μmol m^{-2} s^{-1}) at six virtual sampling points (X_0–X_5) for M-A-35/50/60 and M-V-35/50/60 (Manavgat site). Shaded band = coffee PPFD target 200–400 μmol m^{-2} s^{-1}; dashed line = coffee planting season. (X_0: open-sky reference; X_1–X_5: under-panel.).

For the arid case study site of Harran (Köppen BSh), saffron and black cumin were selected as the target crops. The analyses of black cumin (evaluated against its PPFD band of 350–500 μmol m^{-2} s^{-1}) are presented in Fig. (**9**).

Monthly sub-panel PPFD series were obtained at six virtual sampling locations (X_0–X_5) for the six Harran configurations (H-A-35/50/60; H-V-35/50/60). A systematic cover-ratio effect was observed: increasing CR depresses PPFD across months. At the same time, the V-shaped geometry yields tighter clustering among under-panel traces (more uniform shade) than the A-shaped geometry, which produces two lateral shade lobes and greater intra-row dispersion.

Across scenarios, CR = 35–50 most consistently intersected the target band during the main growing months, with H-A-50 and H-V-50 providing the best balance between seasonal compliance and spatial homogeneity. Under CR = 35, exceedances above 500 μmol m^{-2} s^{-1} occurred in late spring–summer at sun-exposed positions (*e.g.*, corridor-adjacent points), suggesting a mild risk of over-illumination unless spacing/tilt are tuned. Under CR = 60, several traces dipped below 350 μmol m^{-2} s^{-1} in winter–early spring, indicating potential light limitation; this can be mitigated by modestly increasing row pitch, slightly reducing effective coverage, or enhancing ground albedo in V-frames. Moderate coverage (CR ≈ 50) is indicated as the most robust setting for black cumin in Harran, with V-frames conferring greater spatial uniformity and A-frames remaining viable.

Saffron analyses are presented in Fig. (**10**), where monthly sub-panel PPFD at the six virtual sampling locations is compared against the species-specific target band (200–400 μmol m^{-2} s^{-1}) to assess configuration-level suitability.

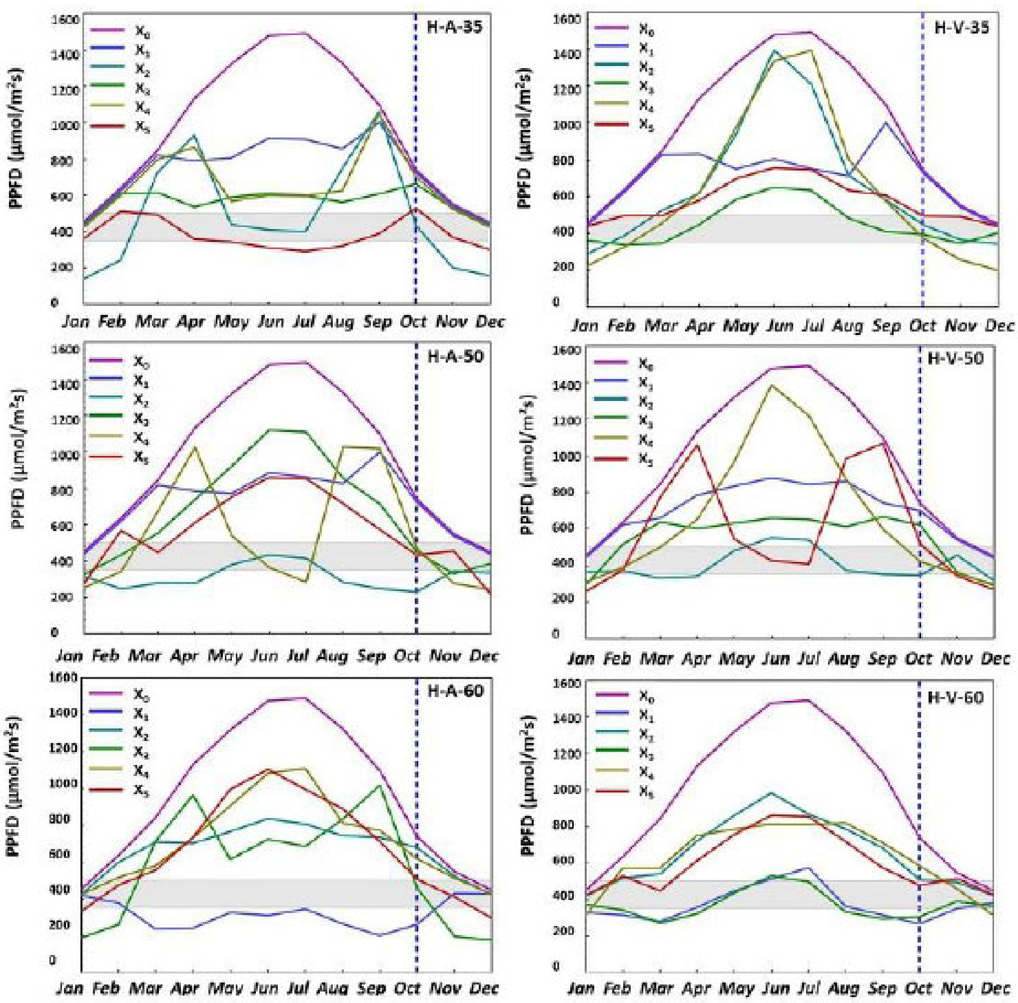

Fig. (9). Monthly sub-panel PPFD (μmol m^{-2} s^{-1}) at six virtual sampling points (X_0–X_5) for H-A-35/50/60 and H-V-35/50/60. Shaded band = black cumin PPFD target 350–500 μmol m^{-2} s^{-1}; dashed line = black cumin planting season. (X_0: open-sky reference; X_1–X_5: under-panel.).

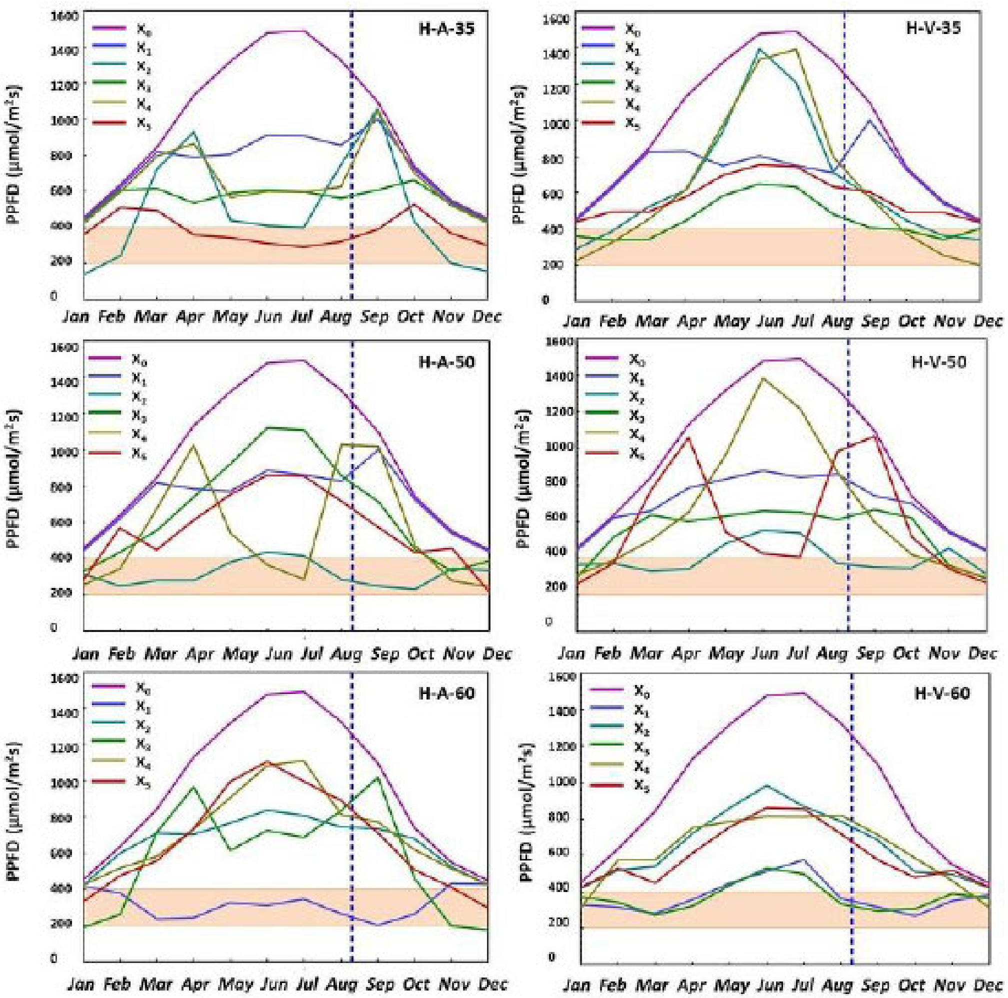

Fig. (10). Monthly sub-panel PPFD (μmol m^{-2} s^{-1}) at six virtual sampling points (X_0–X_5) for H-A-35/50/60 and H-V-35/50/60. Shaded band = saffron PPFD target 200–400 μmol m^{-2} s^{-1}; dashed line = saffron planting season. (X_0: open-sky reference; X_1–X_5: under-panel.).

Monthly sub-panel PPFD series were derived from the ground-irradiance maps at six pre-defined virtual sampling locations (X_0–X_5) for the six Harran configurations (H-A-35/50/60 and H-V-35/50/60). The shaded band denotes the saffron target (200–400 μmol m^{-2} s^{-1}), and the dashed line marks the late-summer planting window. As CR increases, PPFD is systematically depressed across months; V-shaped layouts exhibit tighter clustering among under-panel traces (reflecting the central valley corridor), whereas A-shaped layouts show greater intra-row dispersion due to lateral shade lobes. The open-sky reference (X_0) remains well above the band during spring–summer, confirming the need for shading to achieve agronomic levels.

Table **4** presents the monthly spatial mean PPFD and sample standard deviation calculated across X_1–X_5 for the Harran scenarios. Monthly spatial SD values ranged from 46.3 to 376.2 μmol/m^{2}s, demonstrating substantial seasonal and configuration-dependent variation in under-panel light distribution. The scenario-averaged SD values were 183.8, 212.9, and 211.4 μmol/m^{2}s for H-A-35, H-A-50, and H-A-60, respectively, compared with 173.9, 192.5, and 148.7 μmol/m^{2}s for the corresponding V-shaped configurations. Thus, V-shaped layouts produced lower average spatial dispersion at all three cover ratios, with the clearest improvement observed at CR60. However, individual months, particularly under H-V-50, still exhibited pronounced spatial heterogeneity. The leave-one-point-out sensitivity analysis yielded a median change of 5.2% in the spatial mean, a 95th-percentile change of 14.1%, and a maximum change of 19.4%. These findings indicate that the five-point sampling scheme provides a reasonable estimate of mean under-panel PPFD for preliminary design comparisons while remaining sensitive to localized irradiance extremes.

Table 4. Monthly spatial mean PPFD ± sample standard deviation across the five under-panel sampling locations (X_1-X_5) for A- and V-shaped agrivoltaic configurations in Harran at cover ratios of 35%, 50%, and 60%. X_0 represents the open-sky reference and was excluded from the calculations. Values are expressed in µmol/m²s. The standard deviation represents spatial irradiance heterogeneity within each deterministic simulation rather than replicate or run-to-run uncertainty.

Months	Scenarios					
	H-A-35	H-V-35	H-A-50	H-V-50	H-A-60	H-V-60
Jan	386 ± 124	370 ± 99	374 ± 70	362 ± 70	378 ± 100	382 ± 41
Feb	522 ± 158	438 ± 115	480 ± 146	482 ± 106	458 ± 126	424 ± 120
Mar	684 ± 123	538 ± 183	590 ± 197	600 ± 170	578 ± 196	428 ± 150
Apr	708 ± 236	670 ± 169	728 ± 265	706 ± 257	698 ± 263	562 ± 201
May	568 ± 170	794 ± 162	720 ± 198	710 ± 205	738 ± 263	664 ± 205
Jun	584 ± 226	990 ± 347	772 ± 315	798 ± 370	826 ± 320	746 ± 206
Jul	576 ± 231	956 ± 332	750 ± 334	760 ± 299	808 ± 300	728 ± 176
Aug	646 ± 203	700 ± 130	782 ± 273	756 ± 239	726 ± 255	614 ± 230
Sep	818 ± 278	616 ± 233	748 ± 307	698 ± 249	698 ± 290	524 ± 192
Oct	622 ± 118	504 ± 150	524 ± 194	540 ± 135	526 ± 154	444 ± 134
Nov	446 ± 145	420 ± 119	430 ± 101	434 ± 83	438 ± 133	454 ± 72
Dec	374 ± 124	368 ± 89	374 ± 90	354 ± 67	328 ± 130	388 ± 40

Table 5. Monthly spatial mean PPFD ± sample standard deviation across the five under-panel sampling locations (X_1-X_5) for A- and V-shaped agrivoltaic configurations in Manavgat at cover ratios of 35%, 50%, and 60%. X_0 represents the open-sky reference and was excluded from the calculations. Values are expressed in µmol/m²s. The standard deviation represents spatial irradiance heterogeneity within each deterministic simulation rather than replicate or run-to-run uncertainty.

Months	Scenarios					
	M-A-35	M-V-35	M-A-50	M-V-50	M-A-60	M-V-60
Jan	355 ± 66	352 ± 78	336 ± 108	372 ± 45	347 ± 93	384 ± 53
Feb	493 ± 89	498 ± 104	491 ± 165	519 ± 64	525 ± 72	533 ± 79
Mar	570 ± 135	630 ± 166	498 ± 108	655 ± 158	611 ± 150	552 ± 97
Apr	718 ± 238	620 ± 121	669 ± 248	674 ± 49	615 ± 55	583 ± 106
May	740 ± 146	664 ± 173	708 ± 120	710 ± 46	672 ± 81	691 ± 120
Jun	659 ± 128	701 ± 191	685 ± 152	782 ± 100	706 ± 118	772 ± 202
Jul	709 ± 98	674 ± 172	701 ± 92	792 ± 126	700 ± 121	752 ± 166
Aug	815 ± 288	621 ± 141	737 ± 297	700 ± 70	680 ± 63	630 ± 162
Sep	633 ± 163	675 ± 192	582 ± 166	694 ± 130	616 ± 122	580 ± 64
Oct	597 ± 160	656 ± 151	572 ± 210	619 ± 141	663 ± 125	615 ± 132
Nov	440 ± 94	430 ± 114	451 ± 128	485 ± 55	468 ± 77	503 ± 42
Dec	340 ± 61	328 ± 78	313 ± 104	334 ± 60	332 ± 81	347 ± 68

Table 5 presents the monthly spatial mean PPFD and sample standard deviation calculated across the five under-panel sampling locations (X_1–X_5) for the Manavgat scenarios. Monthly spatial SD values ranged from 42.4 to 297.1 µmol m^{-2} s^{-1}, indicating configuration- and season-dependent variation in the under-panel light environment. The scenario-averaged SD values were 138.9, 140.1, and 158.1 µmol m^{-2} s^{-1} for M-A-35, M-A-50, and M-A-60, respectively, compared with 87.0, 96.6, and 107.6 µmol m^{-2} s^{-1} for the corresponding V-shaped configurations. Accordingly, V-shaped layouts produced lower average spatial dispersion at all three cover ratios, suggesting a more uniform distribution of PPFD beneath the array. The leave-one-point-out sensitivity analysis resulted in a median change of 3.7% in the spatial mean, a 95th-percentile change of 9.4%, and a maximum change of 16.9%. These results indicate that the five under-panel sampling points provide a reasonably stable estimate of mean PPFD for preliminary scenario comparisons, although the higher monthly SD values observed in some configurations confirm that localized irradiance extremes remain relevant. The reported standard deviations describe spatial heterogeneity within a single deterministic simulation and should not be interpreted as replicate-based experimental uncertainty.

When interpreted against the 200–400 μmol m^{-2} s^{-1} criterion, the most persistent compliance during the active autumn–spring period is indicated for CR = 50–60 under both typologies, with V-50/60 yielding the most uniform sub-panel environment and A-50 providing a comparable balance. At CR = 35, exceedances above the upper bound are frequent in late spring, while at CR = 60 occasional dips near/below 200 μmol m^{-2} s^{-1} can occur mid-winter at core-shade points. These shortfalls can be mitigated through minor geometric or optical adjustments (*e.g.*, modestly increased row pitch, slight tilt recalibration, or controlled ground-albedo management). Moderate-to-high coverage (CR ≈ 50–60) is supported as the most suitable range for saffron in Harran, offering seasonally appropriate light levels with improved spatial homogeneity.

5. DISCUSSION

Across both sites and all six configurations, crop-aligned performance was governed by predictable interactions between typology and CR: V-shaped frames generally produced more uniform sub-panel light (*via* a central valley corridor) than A-shaped frames (with lateral shade lobes), while increasing CR systematically depressed PPFD. When interpreted against species-specific targets, saffron in Harran showed potential compatibility at CR ≈ 50–60, black cumin at CR ≈ 35–50, coffee in Manavgat at CR ≈ 50–60, and avocado at CR ≈ 35–50; within these bands, V-frames tended to maintain seasonal compliance more consistently, although A-frames remained viable where tilt, inter-row spacing, and ridge/valley height (θ/S/h) were appropriately tuned. The results therefore suggest that moderate coverage with typology-appropriate geometry offers a promising balance between crop light requirements and water co-benefits, though several important limitations must be acknowledged. First, irradiance values represent monthly aggregates from a single TMY weather file, and inter-annual variability is not captured. Second, the PPFD conversion applies a fixed spectral factor (4.57 μmol J^{-1}) derived for standard solar radiation; spectral shifts caused by partial transmission through module glass or shading may alter effective PPFD, particularly in the blue and red wavebands relevant to photosynthesis. Third, only six sampling points were used; spatial statistics from a full-grid extraction would provide more robust uniformity metrics. Fourth, microclimate variables, canopy temperature, vapor pressure deficit, soil moisture, and wind speed, are not modelled, yet these can substantially modify crop physiological responses even when PPFD is within the target range. Fifth, no crop growth, yield, or PV energy output data were generated, so conclusions on productivity or energy compromise remain speculative. Field validation, continuous PPFD logging, agronomic yield trials, and operational water accounting, is required to confirm these simulation-based findings.

The descriptive spatial statistics provide quantitative support for the observed differences between the A- and V-shaped configurations. In Manavgat, the scenario-averaged spatial standard deviations were consistently lower for the V-shaped layouts (87.0–107.6 μmol m^{-2} s^{-1}) than for the corresponding A-shaped layouts (138.9–158.1 μmol m^{-2} s^{-1}). A similar tendency was observed in Harran, where V-shaped configurations exhibited average SD values of 148.7–192.5 μmol m^{-2} s^{-1}, compared with 183.8–212.9 μmol m^{-2} s^{-1} for A-shaped configurations. This pattern indicates that the central valley geometry generally produces a more spatially uniform under-panel light environment. The improvement was most evident at CR60 in Harran and across all three CR levels in Manavgat. Nevertheless, monthly SD values reached 297.1 μmol m^{-2} s^{-1} in Manavgat and 376.2 μmol m^{-2} s^{-1} in Harran, showing that substantial localized heterogeneity may persist during months even when the annual scenario-level average suggests greater uniformity.

The leave-one-point-out sensitivity analysis further indicated that the estimated spatial means were reasonably stable. Omitting one of the five under-panel points changed the mean by a median of 3.7% in Manavgat and 5.2% in Harran; the corresponding 95th-percentile changes were 9.4% and 14.1%, respectively. However, maximum changes of 16.9% in Manavgat and 19.4% in Harran demonstrate that individual sampling locations can materially affect the estimated mean when strong shade gradients occur. Therefore, the five-point sampling scheme is considered adequate for preliminary comparison and crop-light compatibility screening, but it cannot fully characterize fine-scale irradiance variability. The reported mean ± SD values represent descriptive spatial statistics from deterministic simulations rather than replicate-based experimental uncertainty. Consequently, inferential statistical tests were not applied, and future studies should employ full-grid PPFD extraction or denser field measurements to quantify spatial distributions, confidence intervals, and temporal variability more robustly.

The results from both locations underscore the heterogeneous light environment created by fixed-tilt PV arrays and highlight the necessity of species-specific spatial planning in AgriPV designs. The inclusion of PPFD thresholds alongside simulation-based radiation data provides a practical framework for crop zoning within shared energy-agriculture infrastructure. Accordingly, higher-light-demanding crops such as avocado and black cumin are better suited to the less-shaded perimeter positions (*e.g.*, X_1–X_2), while more shade-tolerant species such as coffee and saffron can be assigned to deeper under-panel positions (*e.g.*, X_3–X_5). This spatial crop allocation strategy can help ensure optimal photosynthetic efficiency and biomass production, thereby enhancing both agricultural and energy land-use efficiency. The findings of this study highlight the potential for expanding AgriPV research through diverse design approaches tailored to a wide range of plant species. Crucial to the effective implementation of such systems is the careful selection of plant species well-suited to the prevailing climatic conditions and the light availability patterns shaped by PV structures. The alignment between solar panel configuration and the PPFD requirements of selected crops must be carefully established to ensure agronomically compatible light environments. It should be noted, however, that PPFD compatibility alone does not guarantee optimal crop performance: temperature, vapour pressure deficit, soil moisture, and canopy microclimate are additional physiological drivers that were not assessed in this simulation and should be addressed in future field studies. Furthermore, while rainwater-harvesting channels are identified as a promising co-benefit of both typologies, no quantitative estimation of harvestable water volume or irrigation savings was made in the present study; such an estimation would require site-specific precipitation data, gutter sizing calculations, and storage-demand matching, and is recommended as a component of future field-validation work. To strengthen the quantitative basis of the results, future iterations of this analysis should report, by crop and scenario, monthly mean PPFD at each sampling point, the percentage of months falling within the species-specific target band, and a spatial uniformity index (*e.g.*, coefficient of variation across X_1–X_5), enabling objective inter-scenario comparison beyond the qualitative pattern descriptions provided here.

This study contributes a structured, simulation-based design framework for AgriPV systems in Türkiye, where field implementations remain limited. By integrating plant-specific PPFD thresholds with parametric structural geometry across two contrasting climates, it provides a replicable methodology for preliminary crop–PV compatibility screening. The results suggest that context-specific typology selection and cover-ratio calibration can simultaneously serve crop light management and renewable energy goals, though this conclusion is conditional on field confirmation of the simulated light environments and their agronomic effects.

CONCLUSION

This simulation study evaluates the potential of AgriPV systems to co-locate solar energy production and high-value crop cultivation in semi-arid and warm-Mediterranean climates, using Türkiye's Harran (Köppen BSh) and Manavgat (Köppen Csa) regions as representative sites. By integrating PPFD simulations with species-specific light requirements, a replicable design framework is proposed to guide preliminary AgriPV system sizing across two structural typologies and three cover ratios. These findings are based solely on simulated irradiance data and should be interpreted as indicative of light compatibility, not as confirmed evidence of crop productivity or energy compromise.

Simulations suggest that moderate CRs (CR = 35–60%) combined with appropriate structural typology selection, A-shaped and V-shaped bifacial PV arrays, can modulate sub-panel light environments toward the PPFD requirements of saffron, black cumin, avocado, and coffee. V-shaped configurations generally showed more spatially uniform shading and better seasonal consistency within target bands, while A-shaped layouts offered practical advantages in maintenance and debris management. Rainwater-harvesting channels are identified as a geometrically compatible co-benefit, though their contribution to irrigation demand reduction requires quantitative field assessment.

These results underscore the importance of site-specific design tailored to local climatic conditions, crop physiology, and structural geometry. The study acknowledges key limitations: irradiance values are monthly aggregates from a single weather-file year; the PPFD conversion uses a fixed spectral factor; microclimate variables (temperature, humidity, VPD) are not modelled; and no crop yield data were generated. These limitations should be addressed through field validation campaigns.

Future work should focus on field validation of the proposed designs, long-term agronomic performance monitoring, and economic feasibility analyses to facilitate broader adoption. With careful implementation, AgriPV can play a pivotal role in advancing sustainable agriculture and the integration of renewable energy in Türkiye and beyond.

AUTHORS' CONTRIBUTIONS

The authors confirm their contribution to the paper as follows: D.K.: Conceptualization, data curation, investigation, methodology, visualization, writing – original draft; D.K.: Investigation, methodology, visualization, software; H.D.Ş.: Investigation, methodology, visualization, software; Ö.Y.: Investigation, methodology, software; T.Ö.: Review & editing. All authors reviewed the results and approved the final version of the manuscript.

LIST OF ABBREVIATIONS

AgriPV	=	Agrivoltaic photovoltaic system
BSh	=	Hot semi-arid climate (Köppen–Geiger classification)
CR	=	Cover ratio
Csa	=	Hot-summer Mediterranean climate (Köppen–Geiger classification)
c-Si	=	Crystalline silicon
EPW	=	EnergyPlus Weather file
GHI	=	Global horizontal irradiance
GIS	=	Geographic information system
MF	=	Reinhart sky subdivision multiplier
MGM	=	Turkish State Meteorological Service (Meteoroloji Genel Müdürlüğü)
PAR	=	Photosynthetically active radiation
PPFD	=	Photosynthetic photon flux density
PV	=	Photovoltaic
SD	=	Standard deviation
SPP	=	Solar power plant
TMY	=	Typical Meteorological Year

TÜİK = Turkish Statistical Institute

VPD = Vapour pressure deficit

ETHICS APPROVAL AND CONSENT TO PARTICIPATE

Not applicable.

HUMAN AND ANIMAL RIGHTS

Not Applicable.

CONSENT FOR PUBLICATION

Not applicable.

AVAILABILITY OF DATA AND MATERIALS

All data generated or analyzed during this study are included in this published article.

FUNDING

None.

CONFLICT OF INTEREST

The authors declare no conflict of interest, financial or otherwise.

ACKNOWLEDGMENTS

Declared none.

REFERENCES

[1] Barron-Gafford GA, Pavao-Zuckerman MA, Minor RL, *et al.* Agrivoltaics provide mutual benefits across the food–energy–water nexus in drylands. Nat Sustain 2019; 2(9): 848-55. http://dx.doi.org/10.1038/s41893-019-0364-5

[2] Soto-Gómez D. Integration of Crops, Livestock, and Solar Panels: A review of agrivoltaic systems. Agronomy 2024; 14(8): 1824. http://dx.doi.org/10.3390/agronomy14081824

[3] Zahrawi AA, Aly AM. A review of Agrivoltaic systems: Addressing challenges and enhancing sustainability. Sustainability 2024; 16(18): 8271. http://dx.doi.org/10.3390/su16188271

[4] Klokov A, Loktionov E, Loktionov Y, Panchenko V, Sharaborova E. A mini-review of current activities and future trends in Agrivoltaics. Energies 2023; 16(7): 3009. http://dx.doi.org/10.3390/en16073009

[5] Rehman A. Towards sustainable agri-photovoltaics through system design and viability in semi-arid conditions. Sol Energy 2025; 299: 113682. http://dx.doi.org/10.1016/j.solener.2025.113682

[6] Lama RK, Jeong H. Design and performance analysis of foldable solar panel for agrivoltaics system. Sensors 2024; 24(4): 1167. http://dx.doi.org/10.3390/s24041167 PMID: 38400325

[7] Yalçın Ö, Kuzyaka D, Özden T. Agrivoltaic system design for sugar beets and wheat in Central Anatolia. Renew Energy 2025; 245: 122800. http://dx.doi.org/10.1016/j.renene.2025.122800

[8] Ali Abaker Omer A, Li M, Zhang F, *et al.* Impacts of Agrivoltaic systems on microclimate, water use efficiency, and crop yield: A systematic review. Renew Sustain Energy Rev 2025; 221: 115930. http://dx.doi.org/10.1016/j.rser.2025.115930

[9] Magarelli A, Mazzeo A, Alhajj Ali S, Ferrara G. Shading enhanced microclimate variability, photomorphogenesis and yield components in a grapevine agrivoltaic system in semi-arid Mediterranean conditions in Puglia region, southeastern Italy. Sci Hortic (Amsterdam) 2025; 350: 114311. http://dx.doi.org/10.1016/j.scienta.2025.114311

[10] Jamil U, Vandewetering N, Pearce JM. Solar photovoltaic wood racking mechanical design for trellis-based agrivoltaics. PLoS One 2023; 18(12): e0294682. http://dx.doi.org/10.1371/journal.pone.0294682 PMID: 38039301

[11] Campana PE, Stridh B, Amaducci S, Colauzzi M. Optimization of vertically mounted agrivoltaic systems. J Clean Prod 2021; 325: 129091. http://dx.doi.org/10.1016/j.jclepro.2021.129091

[12] Riaz MH, Imran H, Younas R, Alam MA, Butt NZ. Module technology for Agrivoltaics: Vertical Bifacial *versus* tilted monofacial farms. IEEE J Photovolt 2021; 11(2): 469-77. http://dx.doi.org/10.1109/JPHOTOV.2020.3048225

[13] Yesilnacar MI, Yenigun I. Effect of irrigation on a deep aquifer: a case study from the semi-arid Harran Plain, GAP Project, Turkey. Bull Eng Geol Environ 2011; 70(2): 213-21. http://dx.doi.org/10.1007/s10064-010-0299-6

[14] Kajikawa N, Uno Y, Kuroki S, *et al.* Effect of Far-red Light on Saffron (<i>Crocus sativus</i> L.) Growth and Crocin Yields. Environ Control Biol 2018; 56(2): 51-7. http://dx.doi.org/10.2525/ecb.56.51

[15] Mzabri I, Rimani M, Charif K, Kouddane N, Berrichi A. Effect of Shade on agro-morphological parameters and weed flora of saffron *(Crocus sativus L.)* Cultivation in the Semiarid Zone of Eastern Morocco. Scientific World J 2022; 2022: 9954404. http://dx.doi.org/10.1155/2022/9954404

[16] Zhou T, Qiu X, Zhao L, *et al.* Optimal light intensity and quality increased the saffron daughter corm yield by inhibiting the degradation of reserves in mother corms during the reproductive stage. Industr Crop Product 2022; 176 http://dx.doi.org/10.1016/j.indcrop.2021.114396

[17] Savaedi Z, Parmoon G, Moosavi SA, Bakhshande A. The role of light and Gibberellic Acid on cardinal temperatures and thermal time required for germination of Charnushka (*Nigella sativa.*) seed. Ind Crops Prod 2019; 132: 140-9. http://dx.doi.org/10.1016/j.indcrop.2019.02.025

[18] Sharifi P, Shirani Bidabadi S. Protection against salinity stress in black cumin involves karrikin and calcium by improving gas exchange attributes, ascorbate–glutathione cycle and fatty acid compositions. SN Appl Sci 2020; 2(12): 2010. http://dx.doi.org/10.1007/s42452-020-03843-3

[19] Kesler S, Kivrak S, Dincer F, *et al.* The analysis of PV power potential and system installation in Manavgat, Turkey—A case study in winter season. Renew Sustain Energy Rev 2014; 31: 671-80. http://dx.doi.org/10.1016/j.rser.2013.12.027

[20] Carr MKV. The water relations and irrigation requirements of Avocado (*Persea americana* Mill.): A review. Exp Agric 2013; 49(2): 256-78. http://dx.doi.org/10.1017/S0014479712001317

[21] Chung SW, Rho H, Lim CK, *et al.* Photosynthetic response and antioxidative activity of 'Hass' avocado cultivar treated with short-term low temperature. Sci Rep 2022; 12(1): 11593. http://dx.doi.org/10.1038/s41598-022-15821-3 PMID: 35804002

[22] Ramalho JC, Pons TL, Groeneveld HW, Azinheira HG, Nunes MA. Photosynthetic acclimation to high light conditions in mature leaves of *Coffea arabica* L.: role of xanthophylls, quenching mechanisms and nitrogen nutrition. Aust J Plant Physiol 2000; 27(1): 43-51. http://dx.doi.org/10.1071/PP99013

[23] DaMatta FM. Ecophysiological constraints on the production of shaded and unshaded coffee: A review. Field Crops Res 2004; 86(2-3): 99-114. http://dx.doi.org/10.1016/j.fcr.2003.09.001

[24] Charbonnier F, le Maire G, Dreyer E, *et al.* Competition for light in heterogeneous canopies: Application of MAESTRA to a coffee (*Coffea arabica L.*) agroforestry system. Agric For Meteorol 2013; 181: 152-69. http://dx.doi.org/10.1016/j.agrformet.2013.07.010

[25] Kottek M, Grieser J, Beck C, Rudolf B, Rubel F. World Map of the

Köppen-Geiger climate classification updated. Meteorol Z (Berl) 2006; 15(3): 259-63.
http://dx.doi.org/10.1127/0941-2948/2006/0130

[26] Taşoğlu E, Öztürk MZ, Yazıcı Ö. High-resolution Köppen–Geiger climate zones of Türkiye. Int J Climatol 2024; 44(14): 5248-65.
http://dx.doi.org/10.1002/joc.8635

[27] Sakin E, Sakin ED, Aslan H. Carbon and Nitrogen Stocks and C: N ratio of Harran Plain Soils. Not Sci Biol 2010; 2(4): 104-10.
http://dx.doi.org/10.15835/nsb245437

[28] Apaydin H, Sonmez FK, Yildirim YE. Spatial interpolation techniques for climate data in the GAP region in Turkey. Clim Res 2004; 28: 31-40.
http://dx.doi.org/10.3354/cr028031

[29] Yetik AK, Arslan B, Şen B. Trends and variability in precipitation across Turkey: A multimethod statistical analysis. Theor Appl Climatol 2024; 155(1): 473-88.
http://dx.doi.org/10.1007/s00704-023-04645-4

[30] Alp Akgül B, Alisinanoğlu F, Fatih Hasoğlu M, Sadettin Özyazıcı M. Maximization of solar radiation for fixed and tracking surfaces in Antalya province of Türkiye. Tehnički glasnik 2023; 17(1): 47-58.
http://dx.doi.org/10.31803/tg-20220426082153

[31] Cengiz AK, Uygur HK. Understanding new consumer trends in turkey through coffee production and consumption in Mardin. Anthropol Noteb 2022; 28: 1-18.
http://dx.doi.org/10.5281/zenodo.7298721

[32] Regional Statistics for Avocado and Black Cumin Between 2022 and 2024. 2024. Available from: https://tuik.gov.tr

[33] Amanpour A, Soltani M, Lipan L, *et al*. Comparative study on nutraceutical and sensorial characteristics of saffron (*Crocus sativus*L.) cultivated in IRAN, SPAIN, and TüRKIYE. J Sci Food Agric 2024; 104(12): 7580-91.
http://dx.doi.org/10.1002/jsfa.13594 PMID: 38775283

[34] McCree KJ. The action spectrum, absorptance and quantum yield of photosynthesis in crop plants. Agricultural Meteorology 1971; 9: 191-216.

DISCLAIMER: Please note that this article is currently in the 'Early view' stage and is not the final 'Version of Record'. While it has been accepted, copy-edited, and formatted, however, it is still undergoing proofreading and corrections by the authors. Therefore, the text may still change before the final publication. Although 'Early view' may not have all bibliographic details available, the DOI and the year of online publication can still be used to cite them. The article title, DOI, publication year, and author(s) should all be included in the citation format. Once the 'Final Version of Record' becomes available the 'Early view' will be replaced by that.